Seismological determination of the physical parameters that govern wave dissipation time and spatial scales

Iñigo Arregui

Andrés Asensio Ramos (IAC, Tenerife, Spain)
David J. Pascoe (University St. Andrews, UK)

Sixth Coronal Loops Workshop
La Roche-en-Ardenne - June 27, 2013

Motivation

We present a method for the determination of the cross-field density structuring of coronal waveguides using the damping of their transverse oscillations

Relevant for MHD seismology

- to infer physical parameters that cannot be directly measured

Relevant for MHD wave heating

Cross-field density structuring determines:

- time/spatial scales for resonant damping of standing/propagating transverse waves
- how fast energy is transferred to small length scales
- Onset of dissipative effects
- Energy carried by the wave
- Fraction of the energy that can be converted into heat

Resonant wave damping

Ionson (1978); Davila (1987); Hollweg & Yang (1988); Sakurai et al. (1991); Goossens et al. (2002); Ruderman & Roberts (2002)

Non-uniform tube **Damping**

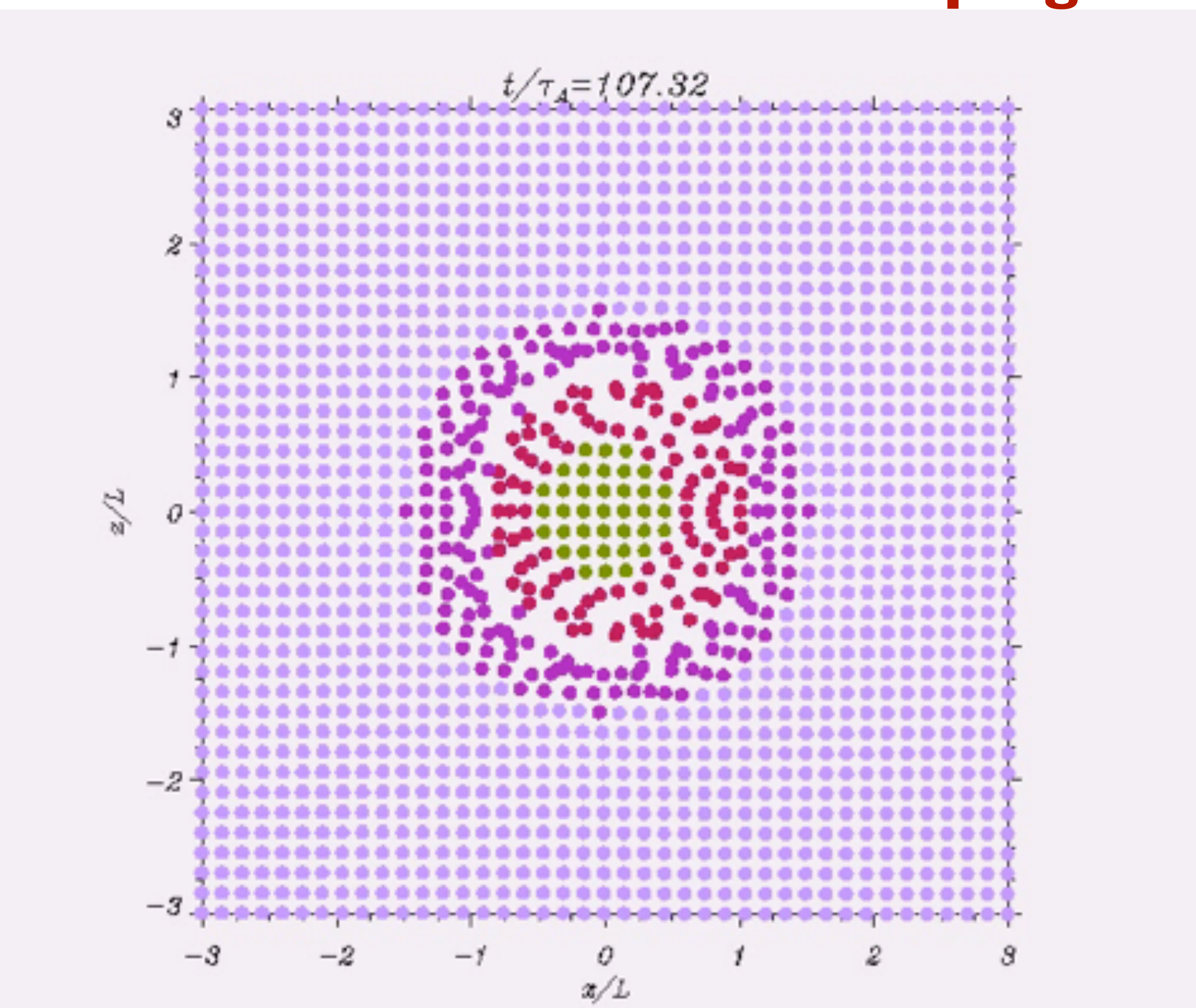

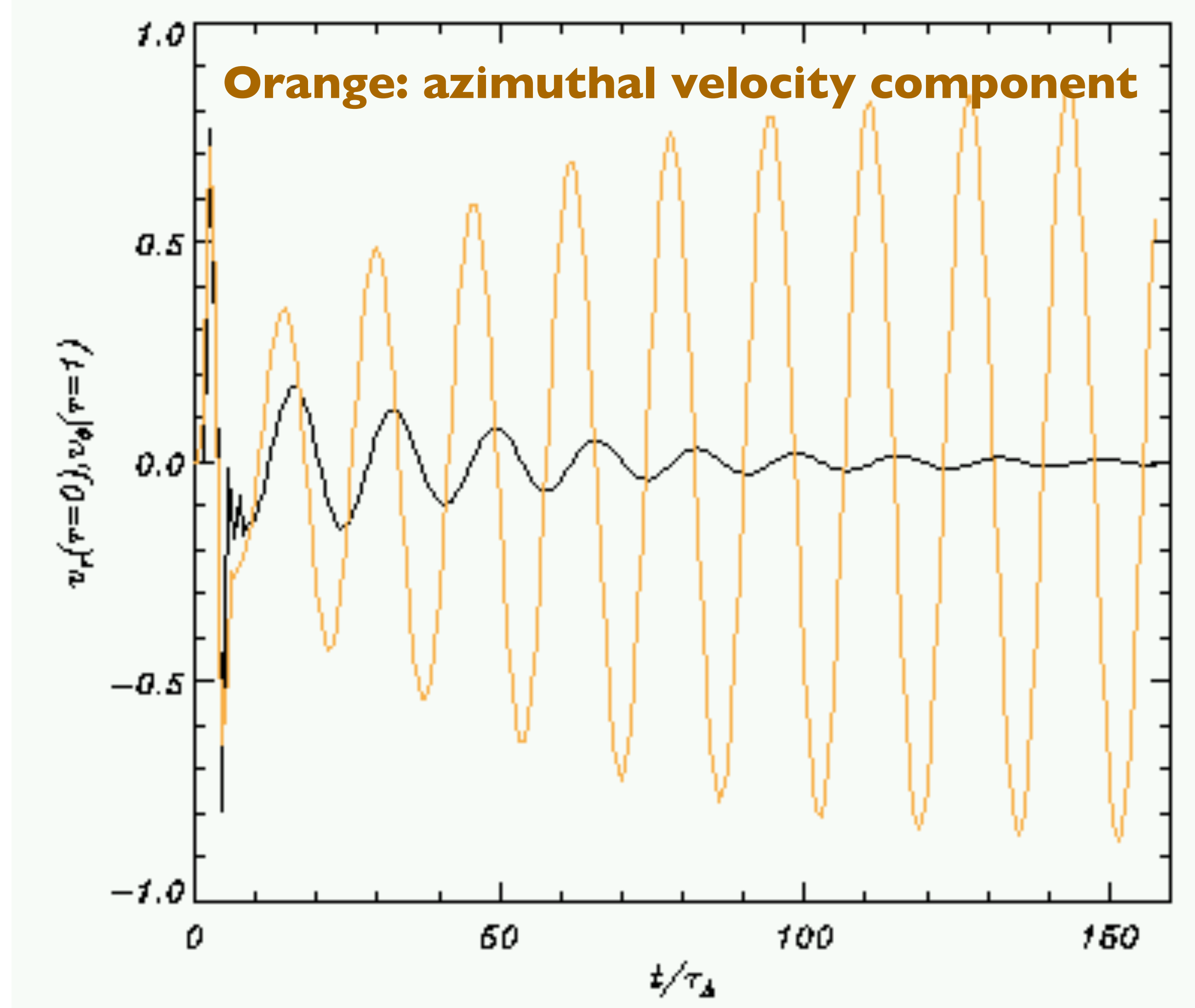

- Smooth density transition at boundary
- Transverse oscillation
- Radial and azimuthal velocity components
- Damping / energy transfer

$$\frac{\tau_d}{P} \sim \left(\frac{l}{R}\right)^{-1} \left(\frac{\zeta+1}{\zeta-1}\right) \qquad \zeta = \frac{\rho_i}{\rho_e}$$

Relevant parameters: ζ $\quad l/R$

Resonant wave damping

Ionson ... ssens et al.

Non-un

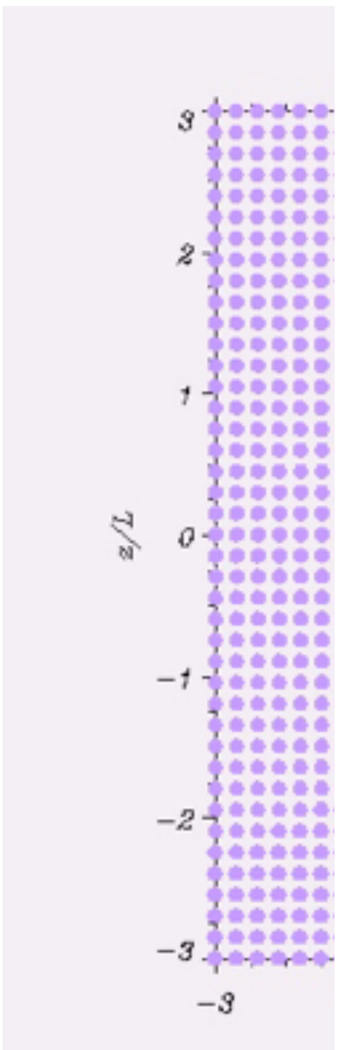

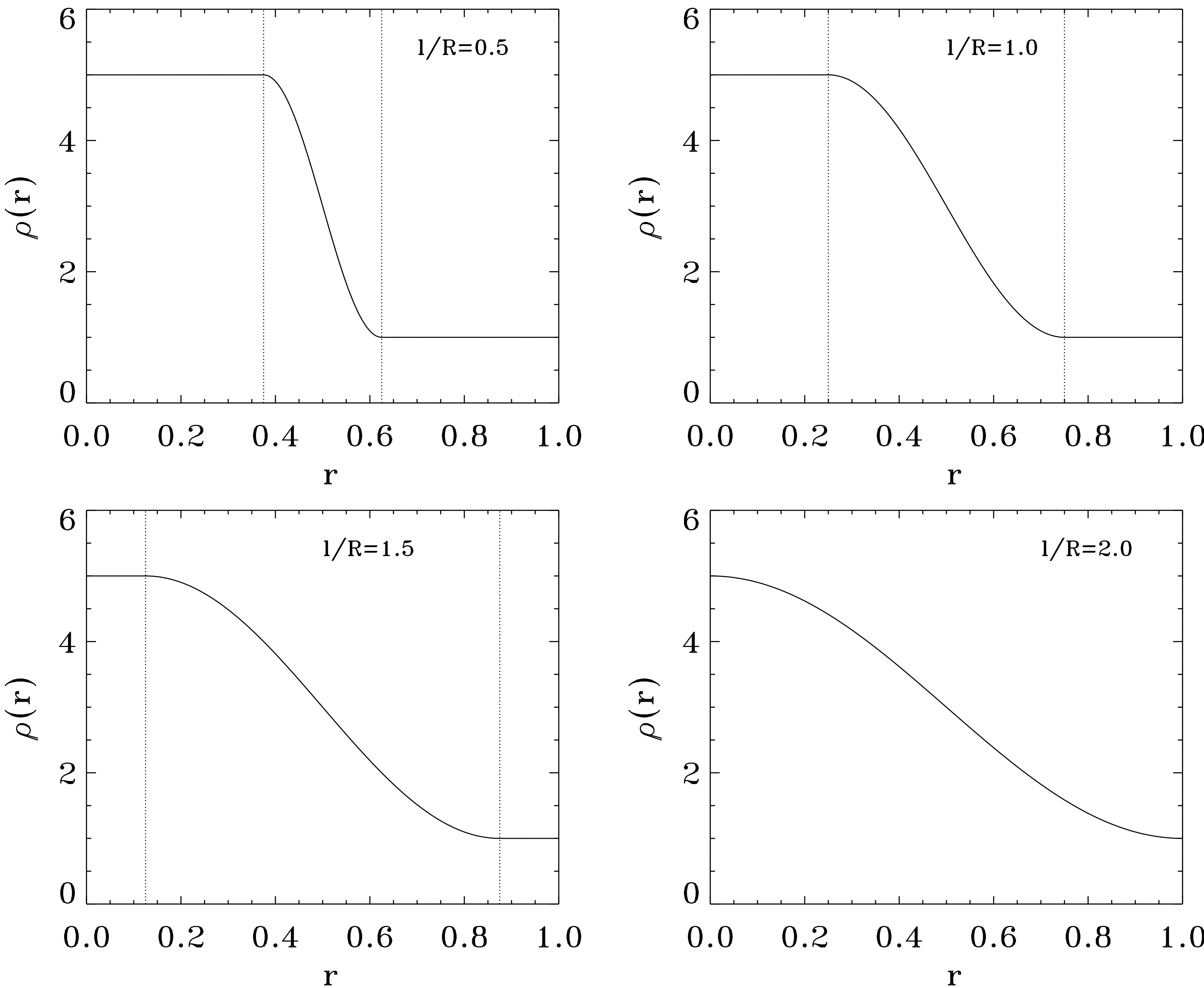

y component

y component

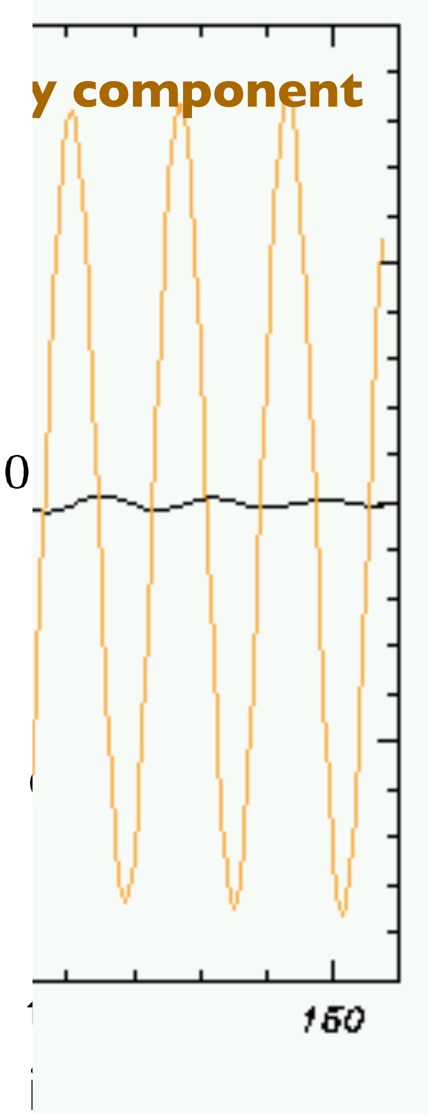

- Smooth
- Transver
- Radial and azimuthal velocity components
- Damping / energy transfer

$$\zeta = \frac{\rho_i}{\rho_e}$$

Relevant parameters: ζ l/R

Energy Transfer and Phase-Mixing of Alfvén Waves

Heyvaerts & Priest (1983); Steinolfson (1985); Parker (1991); Hood et al. (1997,2002); Nakariakov et al. (1997); De Moortel et al. (1999,2000); Ofman & Aschwanden (2002); McLaughlin et al. (2011)

Terradas et al. (2006)

Black: transverse velocity component

Orange: azimuthal velocity component

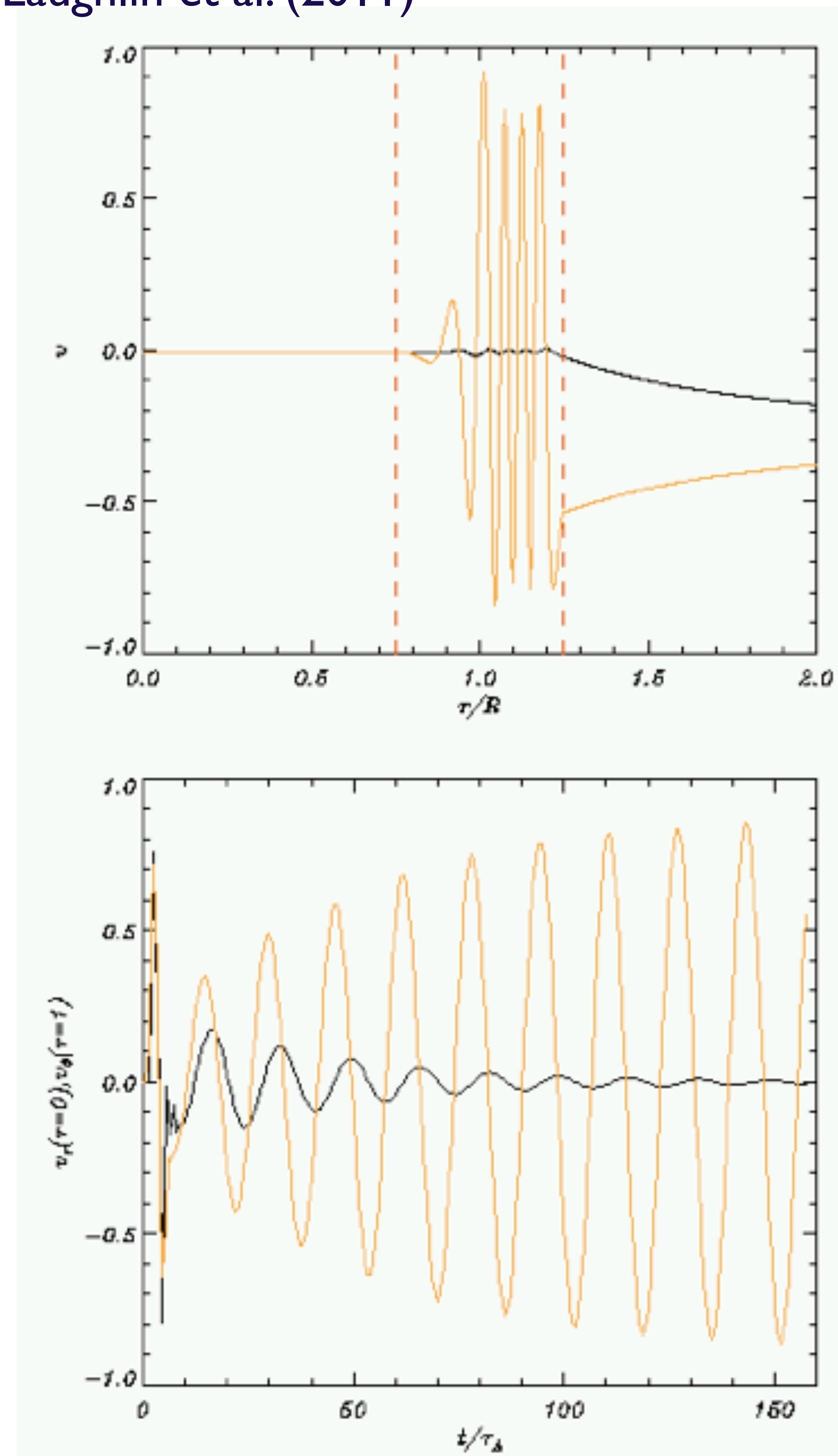

Phase mixing

$$L_{\rm PM} = \frac{2\pi}{\frac{d\omega_{\rm A}}{dr} t}$$

Energy transferred to small length-scales can be dissipated

Enhanced viscous and resistive dissipation

Heating at tube boundary

Thick layers > faster damping, but slower small-scale creation

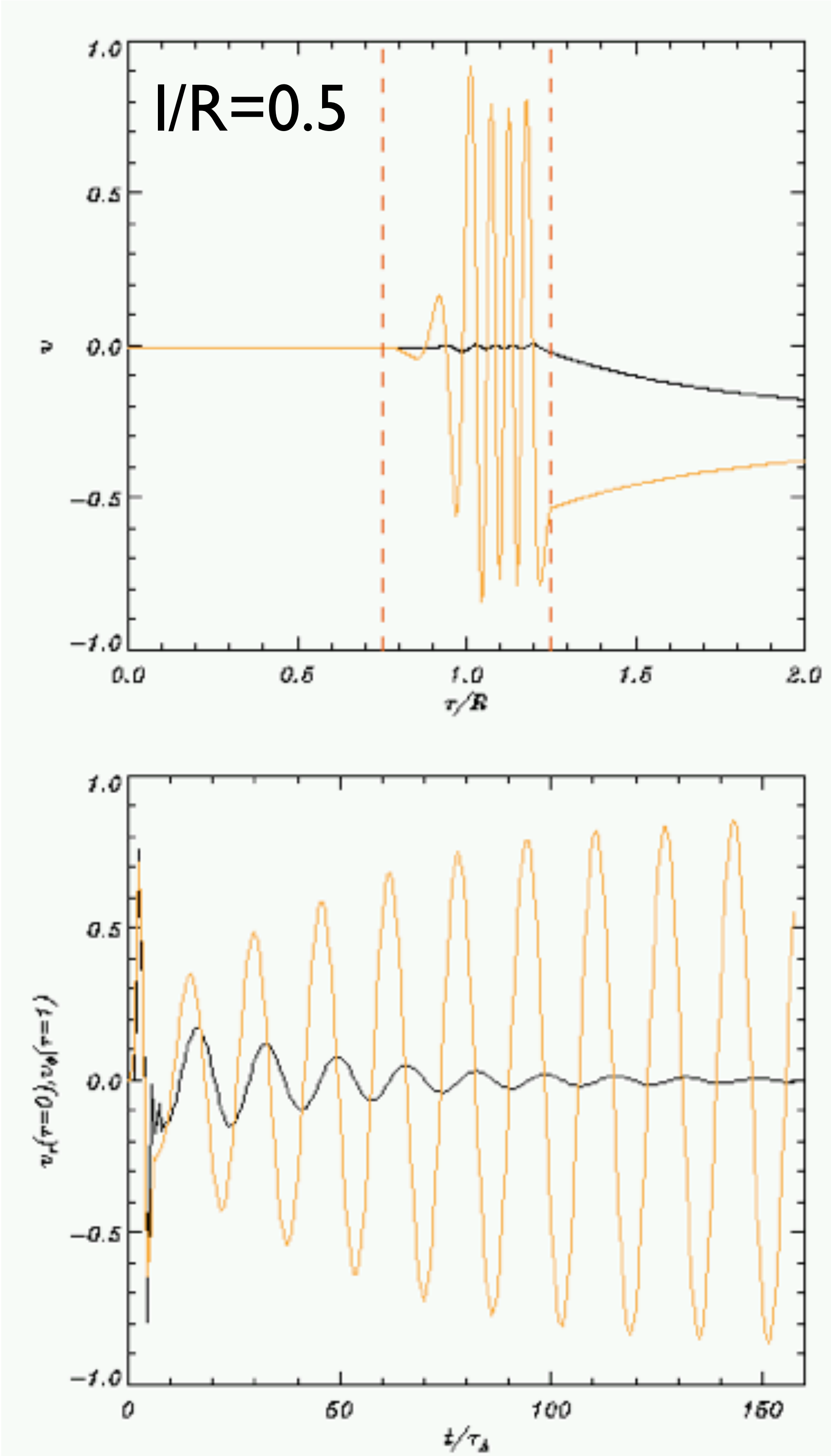

Movies by
J. Terradas

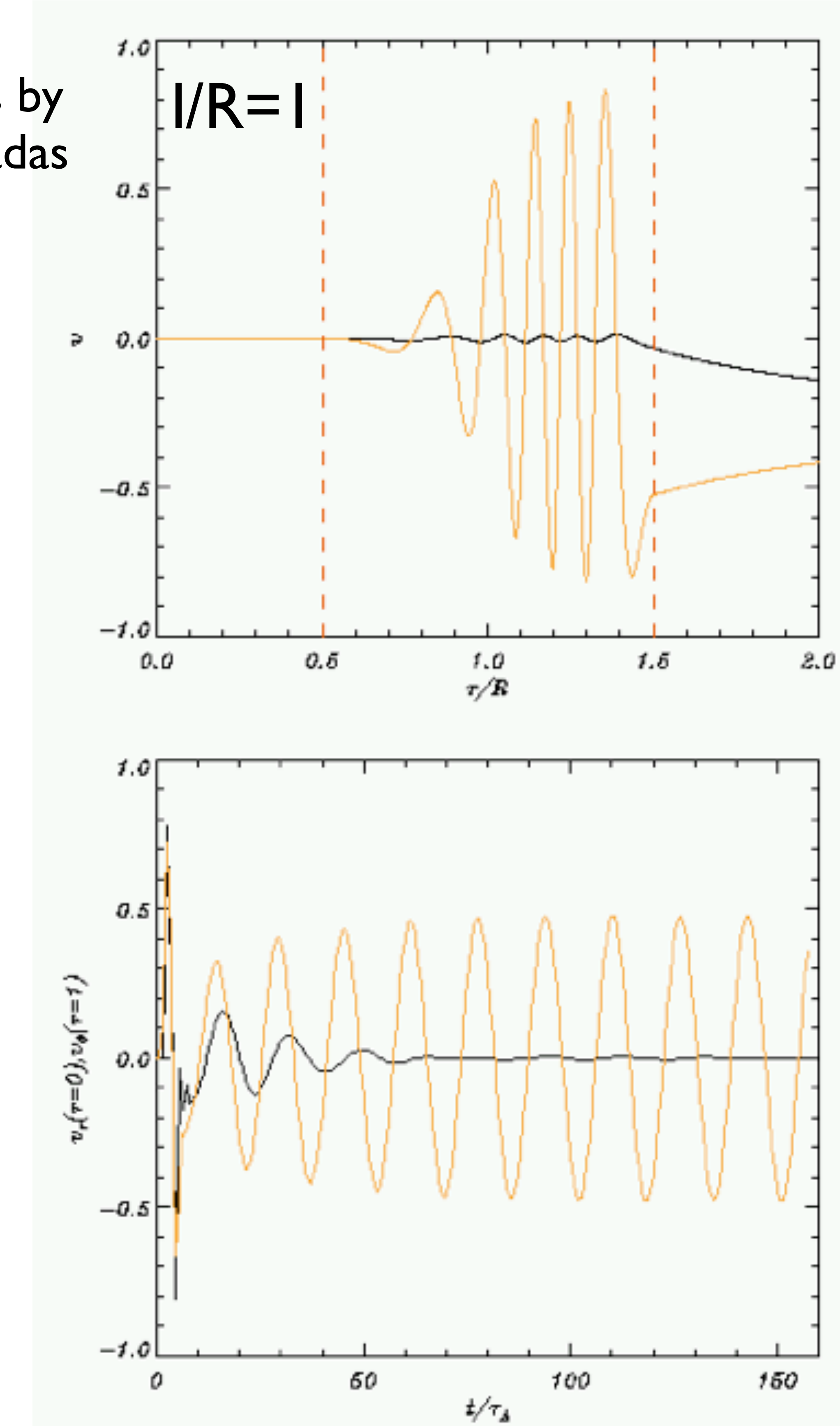

At a given point dissipation becomes important

Relevant time and spatial scales for

wave energy transfer - phase mixing - resistive diffusion

see also Lee & Roberts (1986); Davila (1987)

Resonant damping

$$\tau_{\rm damping} \sim \frac{R}{l}\left(\frac{\zeta+1}{\zeta-1}\right)P$$

Phase-mixing > creation of small scales

$$L_{pm} = 2\pi/(t|\omega_{\rm A}'|)$$

Resistive dissipation important when

$$l_{ra} =\sim (R_{\rm m}|\omega_{\rm A}'|)^{-1/3}$$

This scale is reached in a time

$$t_{ra} = 1/(l_{\rm la}|\omega_{\rm A}'|) = R_{\rm m}^{1/3}|\omega_{\rm A}'|^{-2/3}$$

$R_{\rm m} = 10^{12}$	$R_{\rm m} = 10^{4}$
$l/R = 0.1$	$l/R = 0.1$
$\tau_{damping}/P = 13$	$\tau_{damping}/P = 13$
$t_{\rm diff}/P = 170$	$t_{\rm diff}/P = 0.36$
$l/R = 0.5$	$l/R = 0.5$
$\tau_{damping}/P = 3$	$\tau_{damping}/P = 3$
$t_{\rm diff}/P = 500$	$t_{\rm diff}/P = 1$
NO heating during oscillation	Heating during oscillation

Attempts to determine the relevant parameters

Goossens et al. (2002) $\zeta = 10$ Damping times consistent with observations

No.	$L[m]$	$R[m]$	R/L	$P[s]$	$\tau_{\rm decay}[s]$	l/R
1	1.68e8	3.60e6	2.1e-2	261	870	**0.16**
2	7.20e7	3.35e6	4.7e-2	265	300	**0.44**
3	1.74e8	4.15e6	2.4e-2	316	500	**0.31**
4	2.04e8	3.95e6	1.9e-2	277	400	**0.34**
5	1.62e8	3.65e6	2.3e-2	272	849	**0.16**
6	3.90e8	8.40e6	2.2e-2	522	1200	**0.22**
7	2.58e8	3.50e6	1.4e-2	435	600	**0.36**
8	1.66e8	3.15e6	1.9e-2	143	200	**0.35**
9	4.06e8	4.60e6	1.1e-2	423	800	**0.26**
10	1.92e8	3.45e6	1.8e-2	185	200	**0.46**
11	1.46e8	7.90e6	5.4e-2	396	400	**0.49**

Damped loops are either

- highly inhomogeneous low contrast loops
- less inhomogeneous high contrast loops

Observational values for the damping rate
only give infinite combinations of ζ and l/R

Arregui et al. (2007) - standing waves

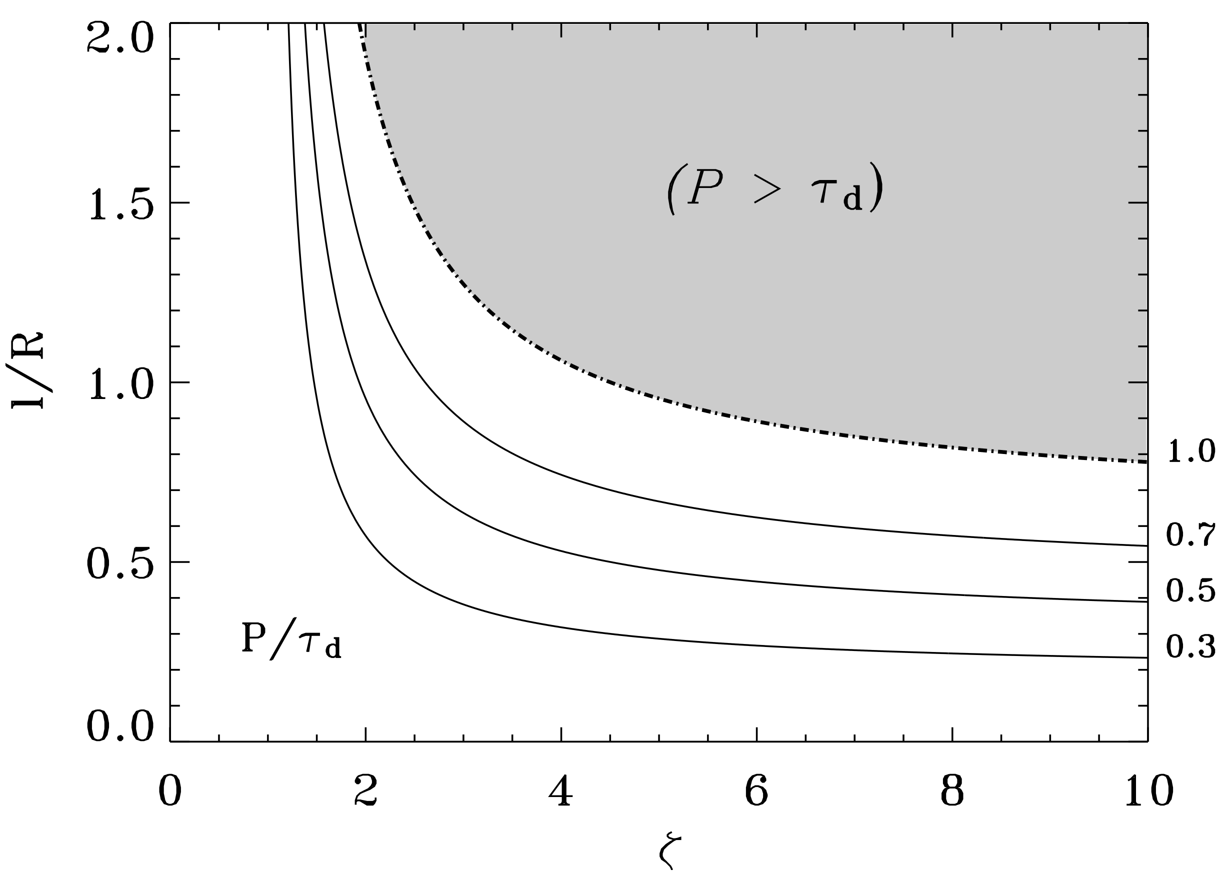

Goossens et al. (2012)
propagating waves

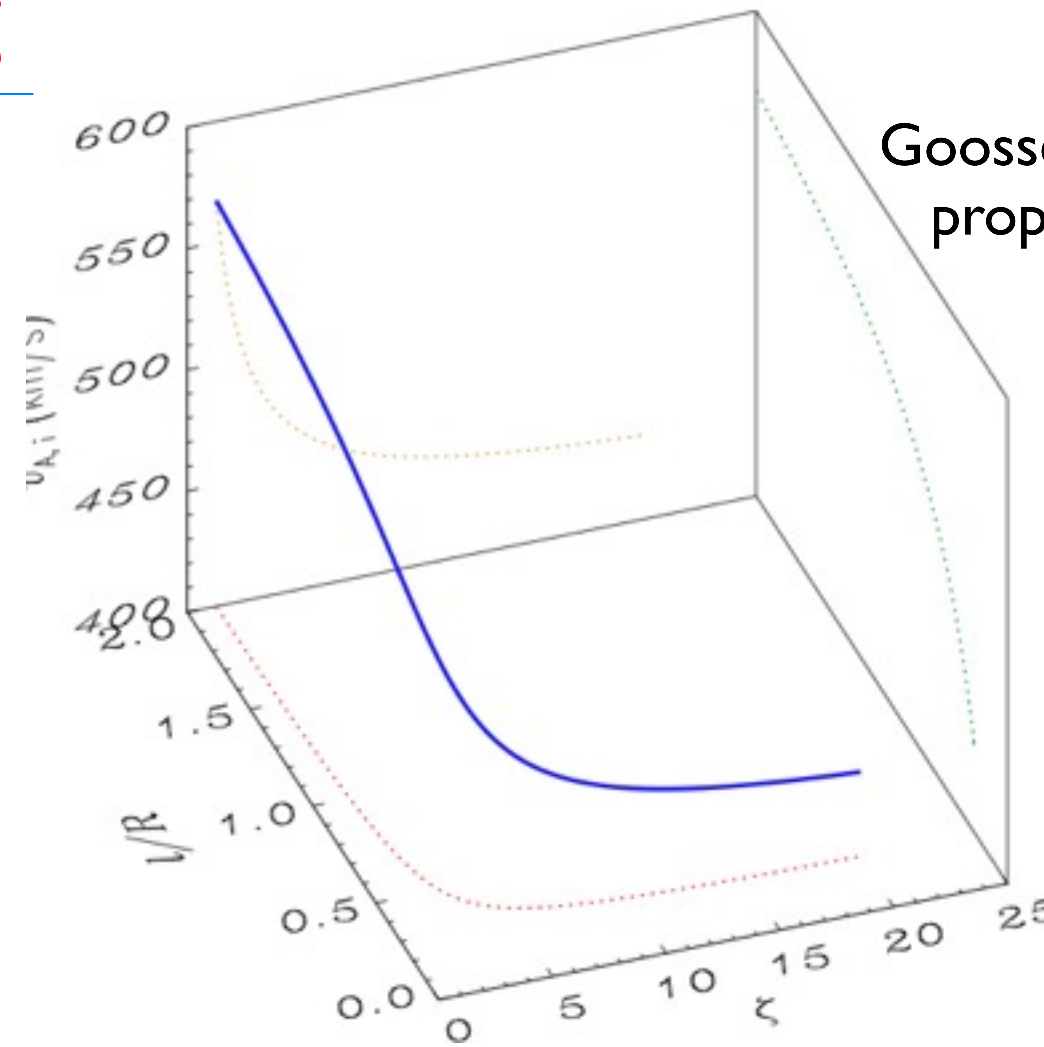

Spatial damping of propagating kink waves

Terradas Goossens & Verth (2010)   see also Soler et al. (2011a,b)   Pascoe, Wright, De Moortel (2010)

For propagating transverse kink waves resonant absorption produces spatial damping

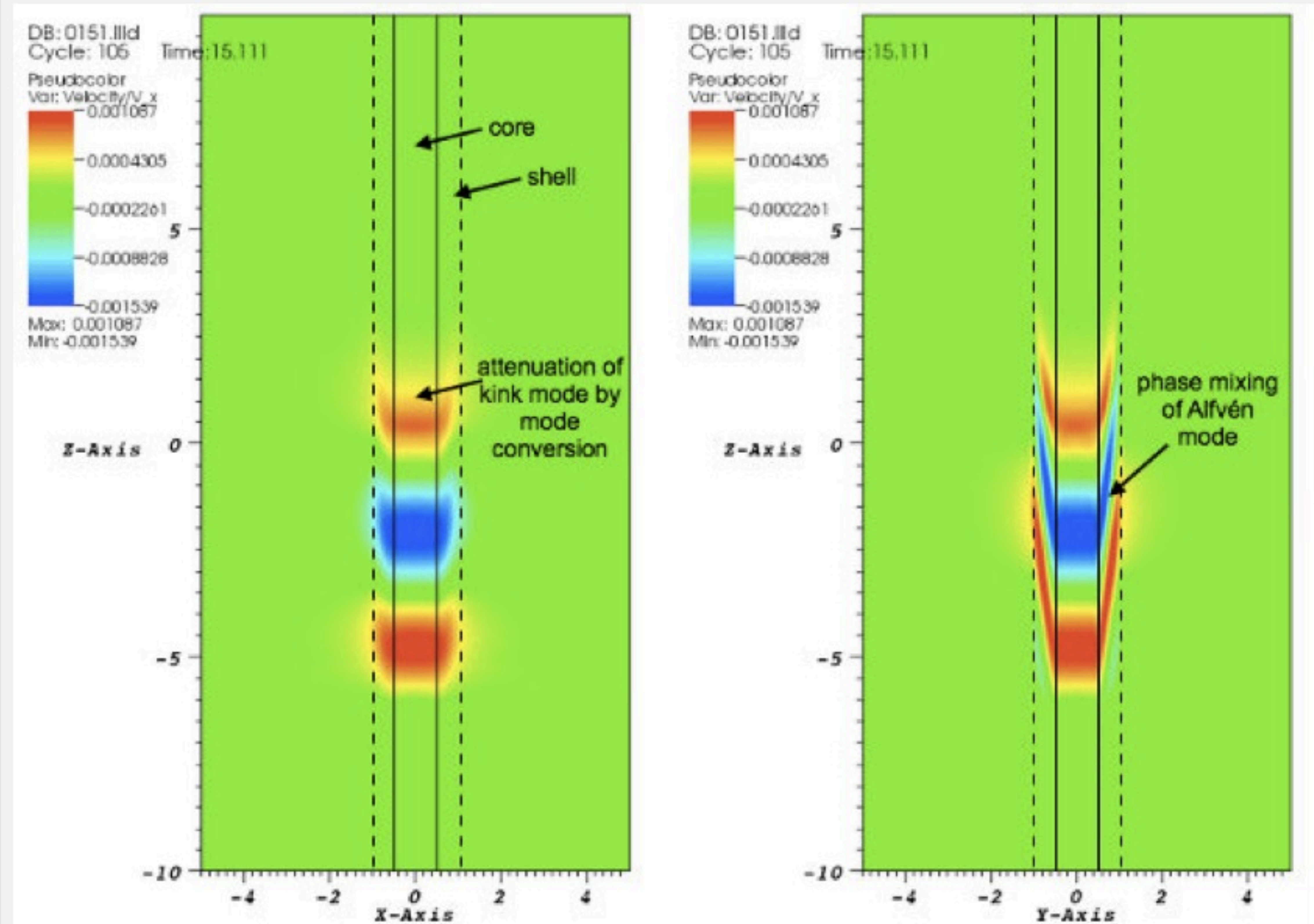

Two damping regimes!

Pascoe et al. (2010, 2011, 2012, 2013)
Numerical simulations

Hood et al. (2013)
Theory: propagating waves

Ruderman & Terradas (2013)
Theory: standing waves

The decay of resonantly damped kink oscillations shows 2 distinct regimes:
Initial Gaussian decay + subsequent exponential damping

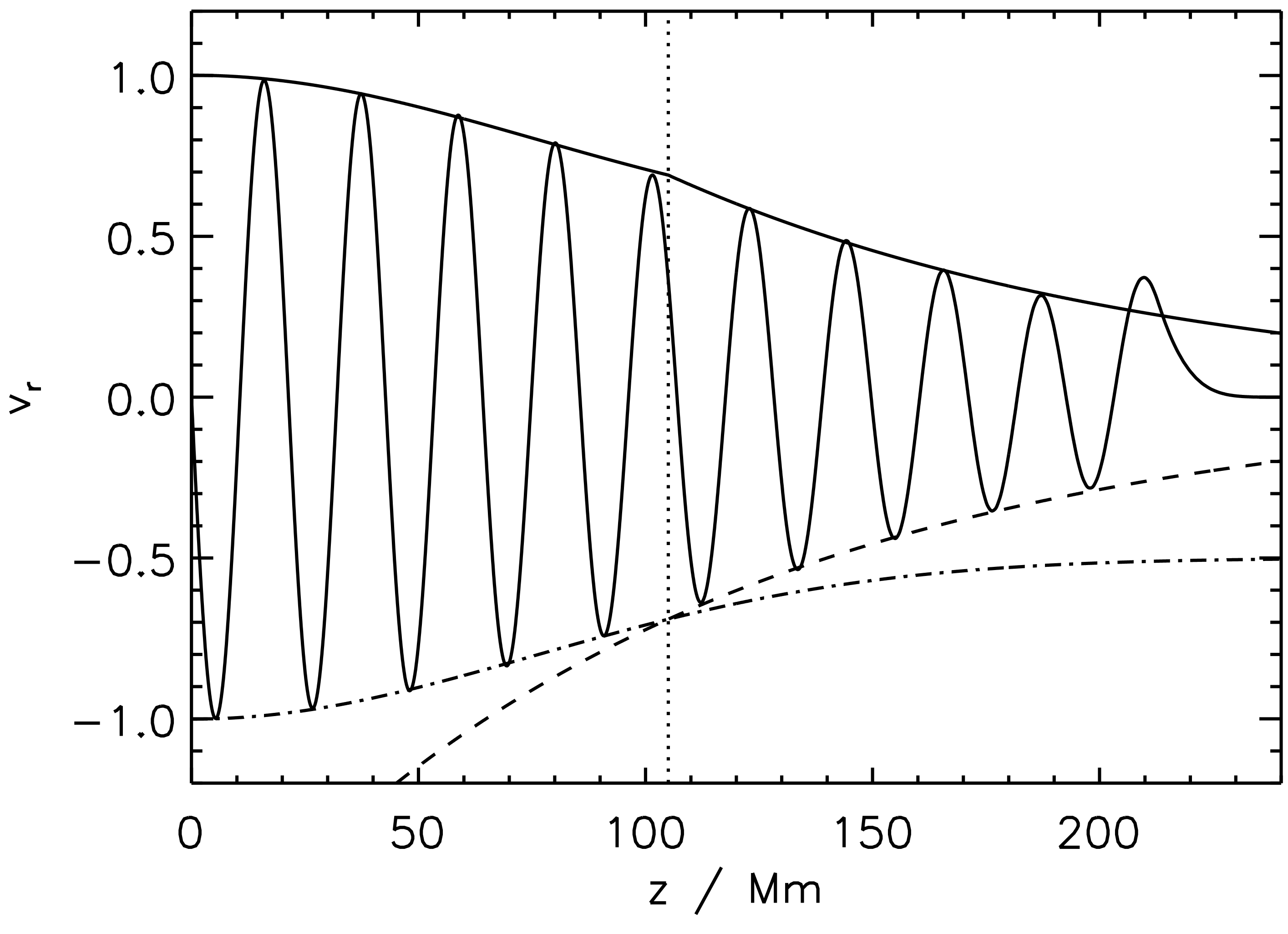

Gaussian damping

$$\frac{L_g}{\lambda} = \left(\frac{2}{\pi}\right)\left(\frac{R}{l}\right)^{1/2}\left(\frac{\zeta+1}{\zeta-1}\right)$$

Exponential damping

$$\frac{L_d}{\lambda} = \left(\frac{2}{\pi}\right)^2\left(\frac{R}{l}\right)\left(\frac{\zeta+1}{\zeta-1}\right)$$

Regime change at location

$$h = \frac{L_g^2}{L_d} = \lambda\left(\frac{\zeta+1}{\zeta-1}\right)$$

Additional information without the need to include new parameters

Bayesian inference with propagating waves

Arregui, Asensio Ramos, & Pascoe (2013, ApJL 769, L34)

Inversion of density contrast and transverse inhomogeneity length scale using Gaussian damping length and height of change of damping regime as data

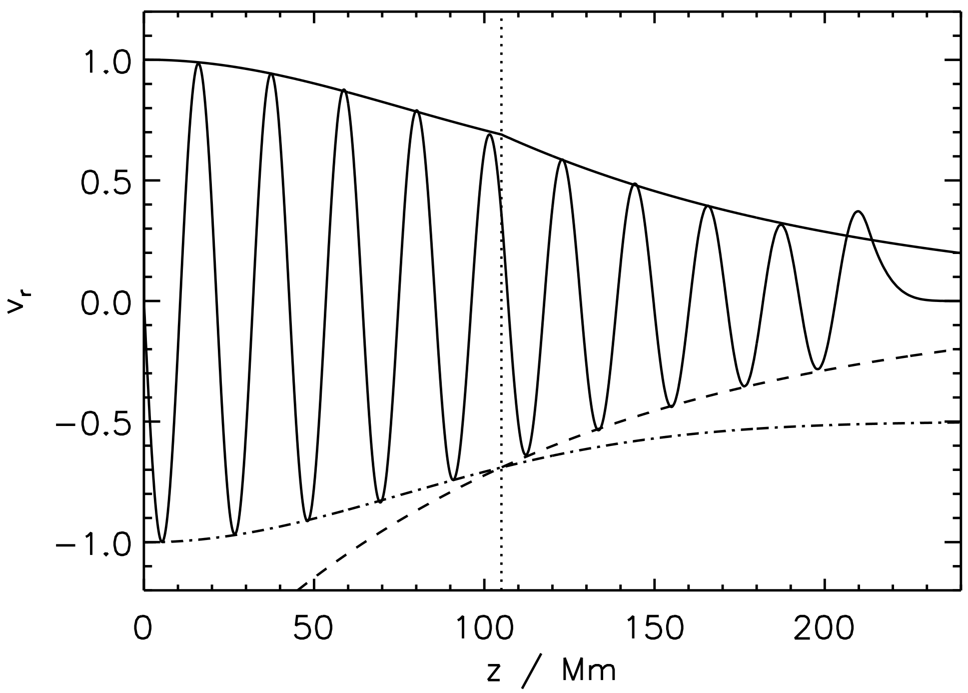

Generate synthetic data using analytical forward model

$$\frac{L_g}{\lambda} = \left(\frac{2}{\pi}\right)\left(\frac{R}{l}\right)^{1/2}\left(\frac{\zeta+1}{\zeta-1}\right) \qquad h = \frac{L_g^2}{L_d} = \lambda\left(\frac{\zeta+1}{\zeta-1}\right)$$

Parameter space

$$\zeta = 1.5, 2, 3, 4 \text{ and } l/R = 0.05, 0.15, 0.2, 0.4$$

Likelihood + uniform priors for contrast and length scale

$$p(d|\boldsymbol{\theta}) = \left(2\pi\sigma_{L_g}\sigma_h\right)^{-1} \exp\left\{\frac{\left[L_g - L_g^{syn}(\boldsymbol{\theta})\right]^2}{2\sigma_{L_g}^2} + \frac{[h - h^{syn}(\boldsymbol{\theta})]^2}{2\sigma_h^2}\right\} \qquad p(\theta_i) = \frac{1}{\theta_i^{max} - \theta_i^{min}} \text{ for } \theta_i^{min} \le \theta \le \theta_i^{max}$$

Use Bayes' rule and marginalise

$$p(\boldsymbol{\theta}|D, M) = \frac{p(D|\boldsymbol{\theta}, M)p(\boldsymbol{\theta}|M)}{\int d\boldsymbol{\theta}\, p(D|\boldsymbol{\theta}, M)p(\boldsymbol{\theta}|M)} \qquad p(\theta_i|d) = \int p(\boldsymbol{\theta}|d)d\theta_1 \ldots d\theta_{i-1}d\theta_{i+1} \ldots d\theta_N$$

Inversion result - example

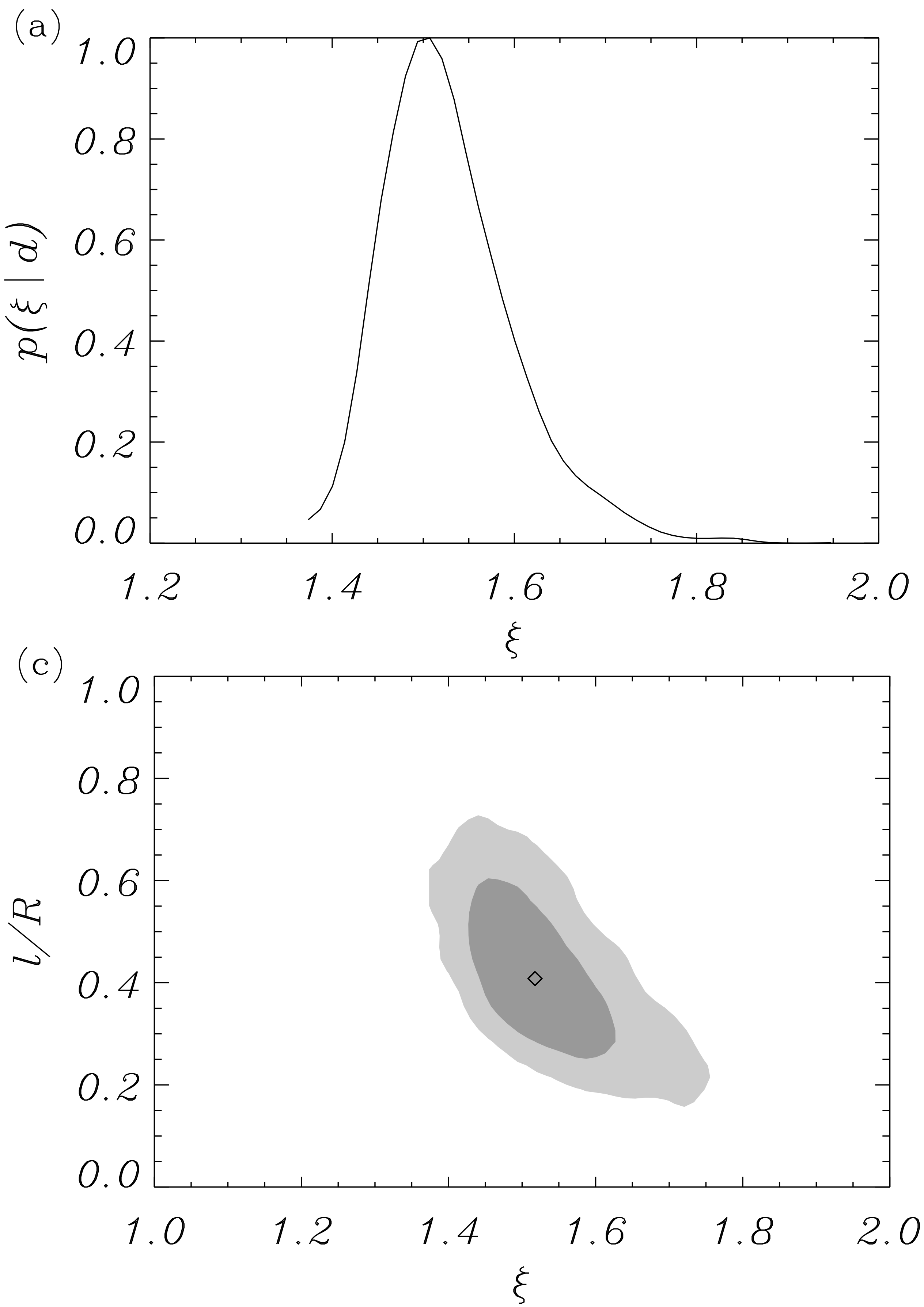

The existence of two damping regimes enables us to constrain the cross-field density structuring

Inversion results

Inversion with analytical forward model

Table 1. Inversion of Synthetic Data Using the Analytical Forward Model

Synthetic Parameters		Synthetic Data		Inversion Results	
ζ	l/R	L_g/λ	h/λ	ζ	l/R
1.5	0.05	14.2	5.0	$1.51^{+0.08}_{-0.06}$	$0.05^{+0.02}_{-0.01}$
1.5	0.15	8.2	5.0	$1.50^{+0.07}_{-0.06}$	$0.16^{+0.05}_{-0.04}$
1.5	0.2	7.1	5.0	$1.51^{+0.07}_{-0.06}$	$0.21^{+0.06}_{-0.05}$
1.5	0.4	5.0	5.0	$1.50^{+0.07}_{-0.05}$	$0.44^{+0.13}_{-0.11}$
3	0.05	5.7	2.0	$3.11^{+0.59}_{-0.38}$	$0.05^{+0.02}_{-0.01}$
3	0.15	3.3	2.0	$3.09^{+0.61}_{-0.40}$	$0.15^{+0.05}_{-0.04}$
3	0.2	2.9	2.0	$3.13^{+0.58}_{-0.41}$	$0.19^{+0.07}_{-0.05}$
3	0.4	2.0	2.0	$3.10^{+0.60}_{-0.41}$	$0.42^{+0.15}_{-0.12}$
4	0.05	4.8	1.7	$4.31^{+1.52}_{-0.79}$	$0.05^{+0.02}_{-0.01}$
4	0.15	2.7	1.7	$4.39^{+1.47}_{-0.85}$	$0.15^{+0.05}_{-0.04}$
4	0.2	2.4	1.7	$4.38^{+1.69}_{-0.85}$	$0.19^{+0.08}_{-0.06}$
4	0.4	1.7	1.7	$4.38^{+1.55}_{-0.86}$	$0.38^{+0.14}_{-0.11}$
10	0.5	1.1	1.2	$11.54^{+4.58}_{-3.88}$	$0.51^{+0.16}_{-0.11}$
10	1.0	0.8	1.2	$11.55^{+4.69}_{-3.81}$	$1.02^{+0.29}_{-0.22}$
10	1.5	0.6	1.2	$12.29^{+4.32}_{-3.89}$	$1.45^{+0.29}_{-0.28}$

Inversion with numerical simulation

Table 2. Inversion of Numerical Data From Simulations

Simulation Parameters		Fitted Data		Inversion Results	
ζ	l/R	L_g/λ	h/λ	ζ	l/R
1.5	0.05	11.5	3.8	$1.73^{+0.12}_{-0.09}$	$0.05^{+0.02}_{-0.01}$
1.5	0.15	7.9	4.6	$1.56^{+0.08}_{-0.07}$	$0.15^{+0.05}_{-0.04}$
1.5	0.2	7.0	4.8	$1.53^{+0.08}_{-0.06}$	$0.21^{+0.07}_{-0.05}$
1.5	0.4	5.0	4.9	$1.52^{+0.07}_{-0.06}$	$0.39^{+0.09}_{-0.08}$
3	0.05	5.5	2.1	$2.88^{+0.46}_{-0.33}$	$0.06^{+0.02}_{-0.02}$
3	0.15	3.5	2.2	$2.74^{+0.44}_{-0.32}$	$0.16^{+0.06}_{-0.04}$
3	0.2	3.1	2.2	$2.74^{+0.41}_{-0.30}$	$0.21^{+0.07}_{-0.05}$
3	0.4	2.1	2.0	$3.09^{+0.57}_{-0.40}$	$0.38^{+0.13}_{-0.11}$
4	0.05	4.9	1.7	$4.17^{+1.32}_{-0.74}$	$0.05^{+0.02}_{-0.01}$
4	0.15	3.1	1.9	$3.19^{+0.64}_{-0.42}$	$0.16^{+0.06}_{-0.05}$
4	0.2	2.7	1.9	$3.33^{+0.74}_{-0.43}$	$0.21^{+0.07}_{-0.06}$
4	0.4	2.3	2.2	$2.73^{+0.43}_{-0.29}$	$0.38^{+0.12}_{-0.10}$

Inversion technique correctly recovers input parameters

Analytical forward model accurate enough when compared to simulation inversions

Large density contrasts represent a challenge from observational point of view

Summary

- The determination of the cross-field density structuring in coronal loops is crucial to assess and quantify the role of MHD waves in heating processes

- We have shown how the existence of two damping regimes for the spatial damping of MHD kink oscillations can be used to determine the density contrast and the transverse inhomogeneity length scale

- Inference is performed in the Bayesian framework, which ensures the problem is solved consistently and with correctly propagated uncertainty

- The observational identification of two damping regimes would also constitute strong support for resonant absorption as a means to damp and contribute to the heating of loops